

## Responses to RC2

We sincerely appreciate the reviewer's positive and constructive comments on our manuscript. We have made careful and thorough modifications according to your suggestions in the revised manuscript. We hope that the revisions meet the reviewer's expectations. The original RC2 comments are shown in *red italics*, followed by our responses in standard black. Key points are highlighted in **bold black**; **Fig.** and **Table** represent the additional figure and table information, respectively.

*This manuscript, titled “Estimating seasonal bulk density of level sea ice using the data derived from in situ and ICESat-2 synergistic observations during MOSAiC”, deals with the sea ice density, one of the key parameter of the sea ice. Sea ice density is indicative of the thermodynamic history of the sea ice, and it plays an essential role in estimating the sea ice thickness during satellite altimetry. However, it is also one of the most poorly observed parameter. So I consider the topic, as well as the major results, are highly relevant to this journal’s scope. A large body of a variety of dataset are used for deriving the IBD, including in-situ, airborne and satellite data. Relevant issues and extensions to the work, such as the impact on satellite altimetry are also covered. I consider the majority of the work is reasonable in its current form. However, I have the following comments for major revisions before it be considered for acceptance.*

**Overall Reply** We would like to express our gratitude for your positive feedback on our manuscript and have made the following major revisions: 1) we clarified the issues of representativeness and independency involved in the regional IBD parameterizations; 2) we analyzed the potential causes of IBD seasonality; 3) We added details describing how to apply the regional IBD parameterizations to satellite retrievals of sea ice thickness, using the AWI CS2 product as an example; 4) We highlighted the improvements in the IBD parameterization itself and the “compensation effect” in the retrieval of sea ice thickness; 5) We discussed the impact of ice deformation on the application of our regional IBD parameterizations.

*First, one key issue is the independency of the estimated IBD and the contributing factors. It is important to differentiate between direct measurements of IBD and the derived IBD. Ideally, only the direct measurements (in this case, coring) should be used for the parameterization of IBD, which however, is not available at large scale. If the derived IBD is used/evaluated, one should be very careful to make sure that it is independent from other parameter used. For example in Eq. 2, IBD is estimated, but not directly observed. One notable example is that the good correlation in Fig. 8.f totally disappears in Fig. 9.f. I wonder whether this contrast can be really explained by the scale of the observation, but not by something else. Is the significant correlation in Fig. 8.f largely due to the way IBD is derived in Eq. 2? Since the ice freeboard is computed as  $(h_f - h_s)$  and the ratio to the ice thickness is directly written in the equation of:  $((h_f - h_s)/h_i)$ , then is the correlation physical, or did it just arise because how you **ESTIMATE** the ice density? One should be very careful here, since uncertainty in the input values could be wrongly interpreted as correlation, since the uncertainty is transferred to the derived value. Then the correlation could be purely artificial. At least some more explanation is needed here. Especially please pay attention to representation issues for DN and L-site studies, which should be at least discussed more thoroughly in Sec. 4.*

**GC1 Reply** We agree with the reviewer's concerns about the representativeness and independency issues associated with the regional IBD parameterizations. We provided additional results to address and clarify these issues. **Overall, we shown that our regional IBD parameterizations remain valid despite the influence of error propagation, see details below.**

**GC1: Representativeness** We clarified the representativeness of the developed IBD parameterizations. Throughout the freezing season, the IBD parameterization derived from the regional buoy sites included a total of 78 samples, with 47 at the DN scale (FYI/SYI = 4/11) and 31 at the L-site scale (FYI/SYI = 4/7), as shown in [Fig. B1](#). In contrast, the local scale comprised 23 samples, including 10 from FYI cores and 13 from SYI cores. The samples used for parameterization themselves exhibited time-varying properties, such as ice porosity, temperature, salinity, thickness, and age. Meanwhile, we focus on comparing *potential* IBD parameterizations derived from regional ([Fig. B2](#); hydrostatic equilibrium method) and local estimates ([Fig. B3](#); weighing), recognizing that absolute robustness cannot be claimed due to inherent differences in their spatial scales, measurement methods, sample sizes, and ice types.

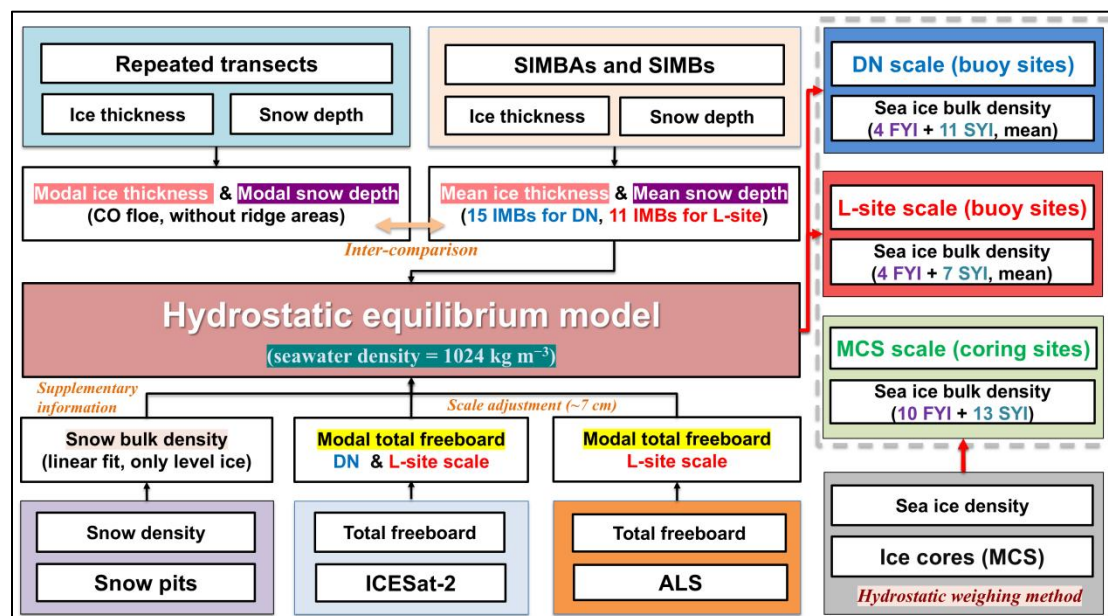


**Figure B1.** Flowchart of the IBD retrieval process.

The parameterized equations for IBD at the regional scale based on sea ice parameters are defined as follows:

$$\overline{\rho_i(x, y, t)} = a1 \times \overline{X(x, y, t)} + a2, \quad (\text{B1})$$

where the  $\overline{\rho_i(x, y, t)}$  and  $\overline{X(x, y, t)}$  represent the regional IBD and other sea ice parameters at any given grid cell over tens of kilometers ( $x, y$ ) and time ( $t$ ), respectively. [Table B1](#) lists the regression coefficients and their 95 % confidence intervals for Eq. (B1).

The parameterized equations for IBD at the local scale based on sea ice parameters are defined as follows:

$$\rho_i(x, y, t) = a1 \times \left(\frac{1}{X(x, y, t)}\right)^{a2} + a3, \quad (\text{B2})$$

where the  $\rho_i(x, y, t)$  and  $X(x, y, t)$  represent the local IBD and other sea ice parameters at any given site ( $x, y$ ) and time ( $t$ ), respectively. [Table B2](#) lists the regression coefficients and their 95 % confidence intervals for Eq. (B2).

**Table B1.** Regression coefficients of the parameterized equations based on sea ice parameters at the regional scale ( $\text{kg m}^{-3}$ ), and parentheses represent 95 % confidence intervals for the regression coefficients.

$\overline{X(x, y, t)}$	Variable type	a1	a2	Input range
Sea ice freeboard (m)	<i>Univariate</i>	-127 (-204, -51)	923 (915, 932)	0.05–0.15 m
Ice freeboard-to-total freeboard ratio	<i>Bivariate</i>	-115 (-158, -71)	950 (935, 966)	0.25–0.45
Ice freeboard-to-thickness ratio	<i>Bivariate</i>	-953 (-1036, -870)	980 (974, 986)	0.05–0.09

**Table B2.** Regression coefficients of the parameterized equations based on sea ice parameters at the local scale ( $\text{kg m}^{-3}$ ), and parentheses represent 95 % confidence intervals for the regression coefficients.

$X(x, y, t)$	Variable type	a1	a2	a3	Input range
Sea ice thickness (m)	<i>Univariate</i>	-0.6 (-1.7, 0.6)	4 (2, 7)	912 (910, 914)	0.4–2.2 m
Sea ice draft (m)	<i>Univariate</i>	-0.4 (-1.2, 0.4)	4 (2, 7)	912 (910, 913)	0.4–2.0 m
Total thickness (m)	<i>Bivariate</i>	-0.7 (-2.1, 0.7)	5 (2, 8)	912 (910, 914)	0.5–2.3 m

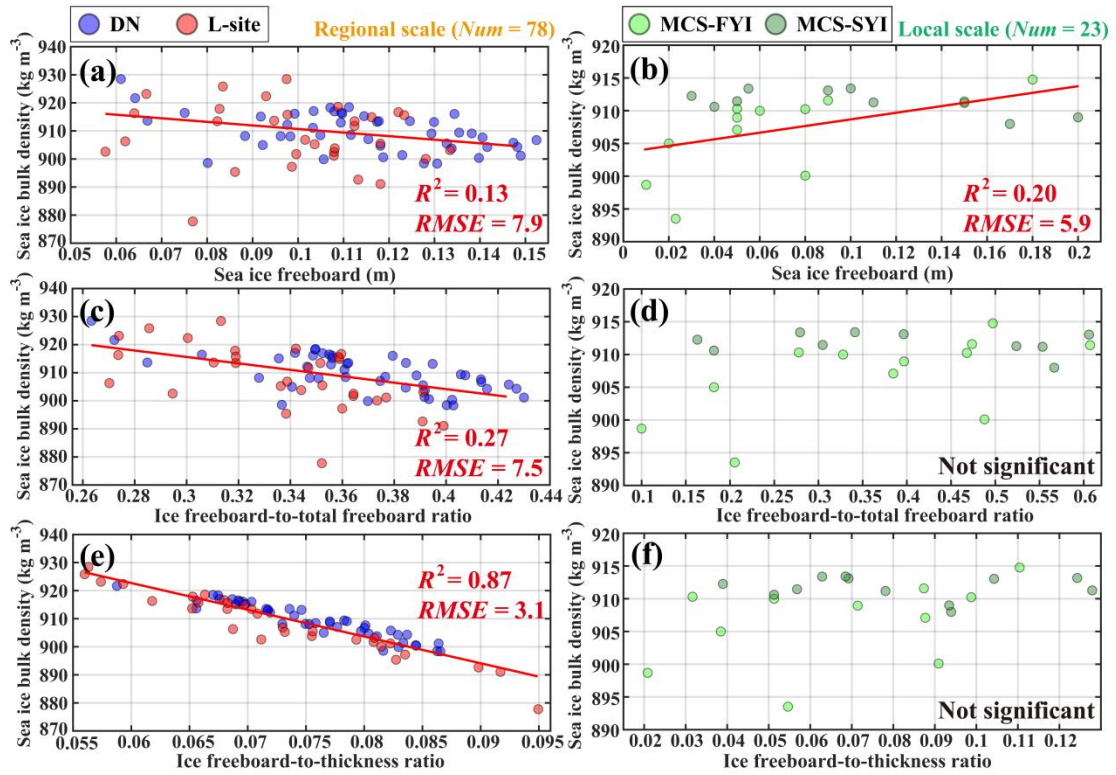


**Figure B2.** Potential parameterizations for IBD at the regional scale and comparison with results at the local scale, including regression models using (a, b) sea ice freeboard, (c, d) ice freeboard-to-total freeboard ratio, and (e, f) ice freeboard-to-thickness ratio. Each panel shows model fit metrics, including the coefficient of determination ( $R^2$ ) and root mean square error ( $RMSE$ , unit:  $\text{kg m}^{-3}$ ). The significance level for the statistical test is set at 95%. The total number of samples ( $Num$ ) is 78 for the regional scale and 23 for the local scale.

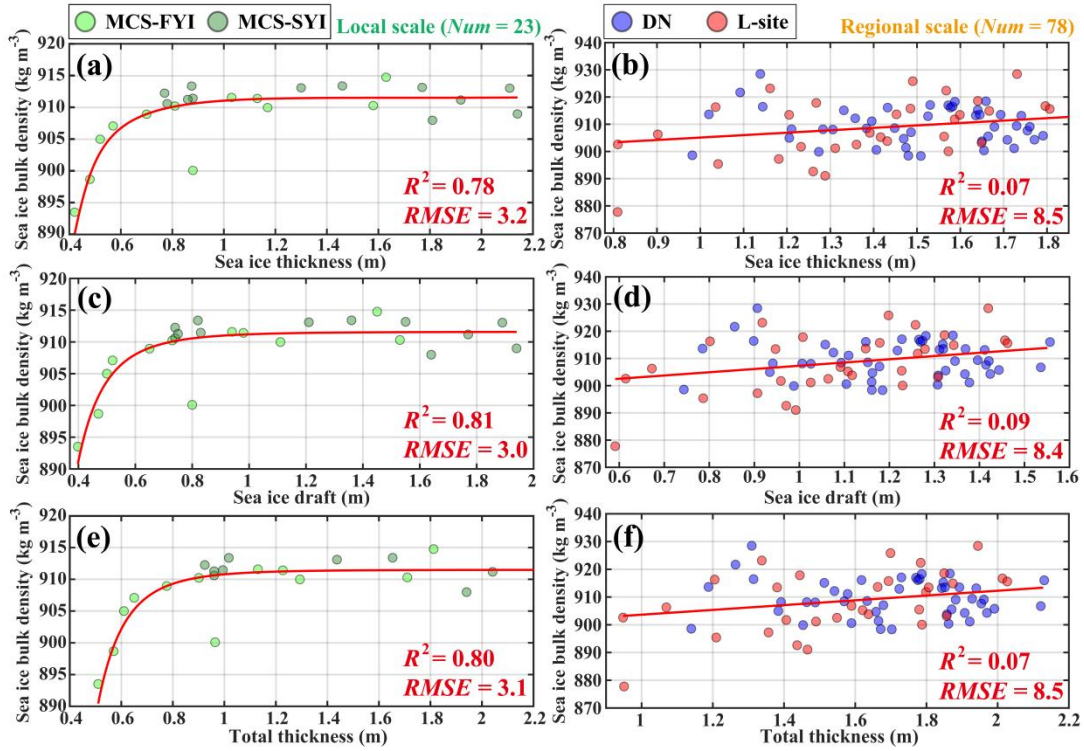


**Figure B3.** Potential parameterizations for IBD at the local scale and comparison with results at the regional scale, including regression models using (a, b) sea ice thickness, (c, d) sea ice draft, and (e, f) total thickness. Each panel shows model fit metrics, including the coefficient of determination ( $R^2$ ) and root mean square error (RMSE, unit: kg m<sup>-3</sup>). The significance level for the statistical test is set at 95%. The total number of samples ( $Num$ ) is 23 for the local scale and 78 for the regional scale.

**GC1: independency issues** We presented several pieces of evidence that the error propagation from different input parameters in Eq. (2) **has not obscured the potential physical phenomena** revealed by the regional IBD parameterizations. Overall, we suggest that these regional IBD parameterizations, which are representative of the hydrostatic equilibrium-based IBD, and the regression coefficients derived from observations, still provide valuable guidance for satellite retrievals of sea ice thickness. **Four main arguments are presented below:**

1) The input parameters in Eq. (2) were independent of each other and exhibited relatively high measurement precision (Section 2.1). Meanwhile, the distinct seasonality observed in these parameters, together with the good agreement in both magnitude and seasonality between the derived IBDs and direct measurements (**Fig. B4**), effectively supports the validity of the developed parameterizations based on these parameters.

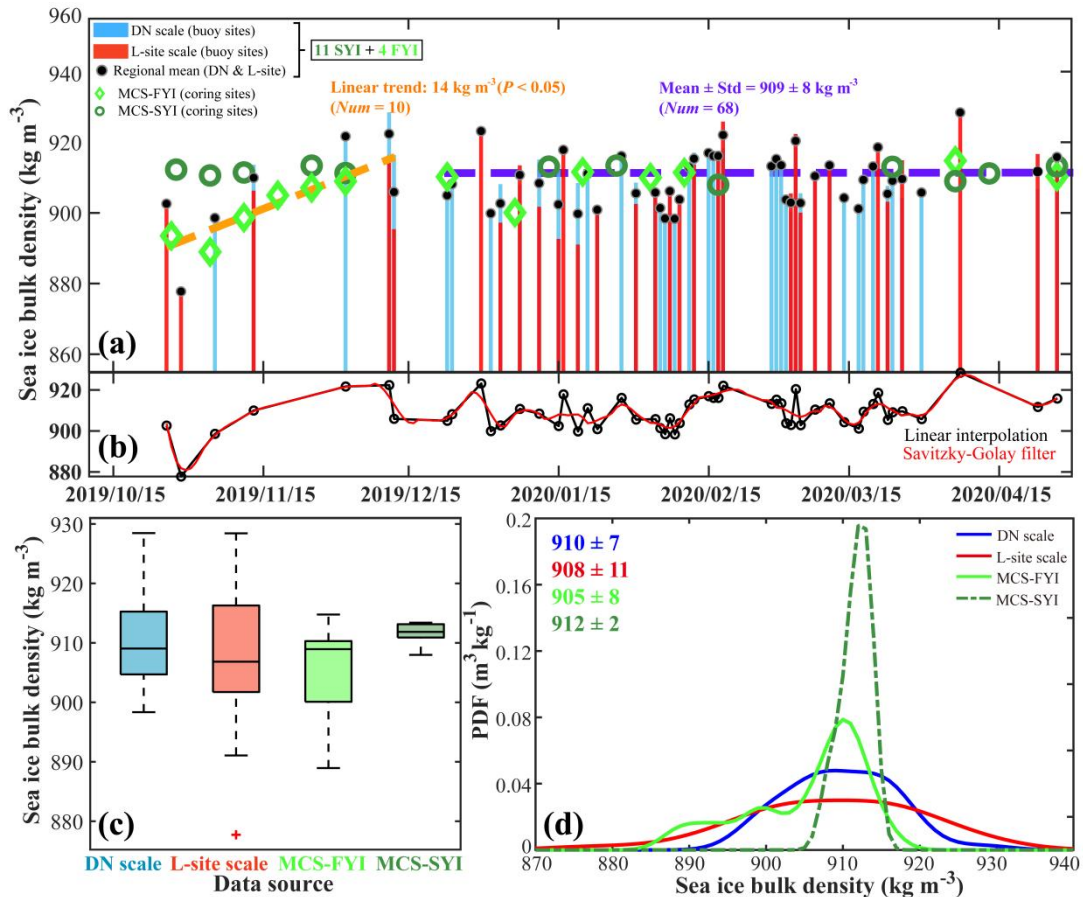


**Figure B4.** (a) Seasonal variation of IBD estimates at the DN (blue bars), L-site (red bars), and MCS (green symbols) scales during the MOSAic freezing season. The black dots are the regional mean of the DN and L-site estimates. The orange dashed line represents the linear fitting from late October to early December ( $R = 0.62$ ,  $P < 0.05$ ) and the purple dashed line indicates the mean  $\pm$  one standard deviation from late December to April. (b) Linear interpolation (black) and smoothing (red) of regional IBD estimates. (c) Box plots of all IBD estimates over the study period, showing interquartile range (IQR, Q3–Q1, boxes), median (black lines), and outliers (greater than  $1.5 \times$  IQR, red crosses). (d) Probability density distribution (PDF) of all IBD estimates over the study period, with labelled values showing the mean  $\pm$  one standard deviation.

2) We used high-precision, spatially coincident airborne measurements from AWI IceBird to further investigate the relationship between ice freeboard-to-thickness ratio and IBD at a spatial resolution of  $25 \text{ km} \times 25 \text{ km}$ . We identified a **similar negative linear function** (Fig. B5) in the same range as Eq. (B1), which is expected to be less affected by error propagation, thus strengthening our conclusions.

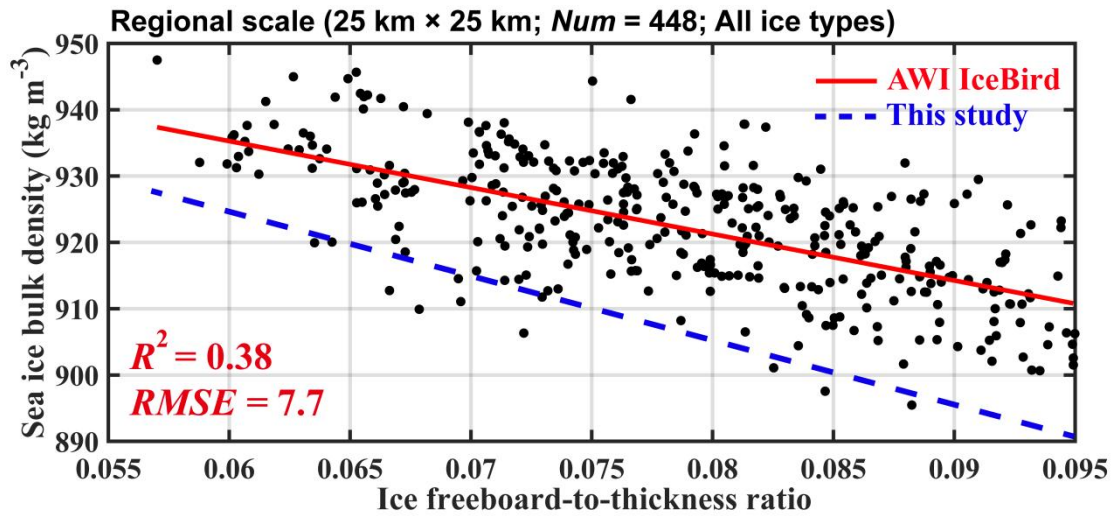


**Figure B5.** Relationship between ice freeboard-to-thickness ratio and IBD at a spatial resolution of  $25 \text{ km} \times 25 \text{ km}$  based on AWI IceBird measurements. The model fit metrics include the coefficient of determination ( $R^2$ ) and root mean square error ( $RMSE$ , unit:  $\text{kg m}^{-3}$ ). **Note:** The significance level for the statistical test is set at 95% and the total number of samples is 448.

3) By incorporating the physical factor of sea ice bulk temperature into the regional IBD parameterizations based on sea ice parameters, we found significant improvements in fitting performance compared to the original models (Fig. B6). This suggests that the initial good fit between different sea ice parameters and IBD is **unlikely to be dominated by computational redundancy or spurious correlations**; otherwise the inclusion of independent physical information would tend to weaken model performance.

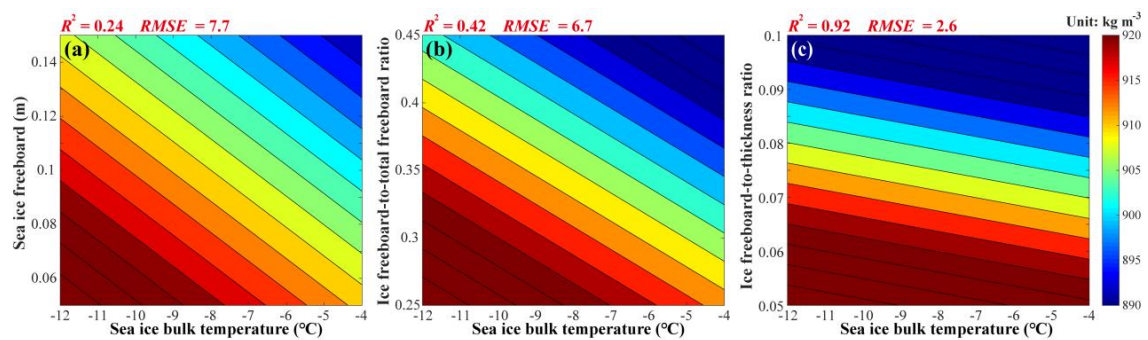


**Figure B6.** Potential parameterizations for IBD at the regional scale using both sea ice parameters and sea ice bulk temperature, including (a) sea ice freeboard and sea ice bulk temperature versus IBD, (b) ice freeboard-to-total freeboard ratio and sea ice bulk temperature versus IBD, (c) ice freeboard-to-thickness ratio and sea ice bulk temperature versus IBD. Each panel shows model fit metrics, including the coefficient of determination ( $R^2$ ) and root mean square error ( $RMSE$ , unit:  $\text{kg m}^{-3}$ ). **Note:** The significance level for the statistical test is set at 95% and the total number of samples is 78.

4) Independent validation with coring samples from the 2022 GoNorth expedition showed that the relative error of our parameterizations was between 0.2% and 0.9% within their applicability range (Fig. B7), and that the regional IBD parameterizations even outperformed the local parameterizations developed from the MOSAiC ice cores. Furthermore, the A10 configuration ( $882 \text{ kg m}^{-3}$ ) significantly underestimated the observed SYI bulk density, while our newly proposed age-related IBD climatology ( $907 \text{ kg m}^{-3}$ ) was significantly improved (see details in GC3 Reply).

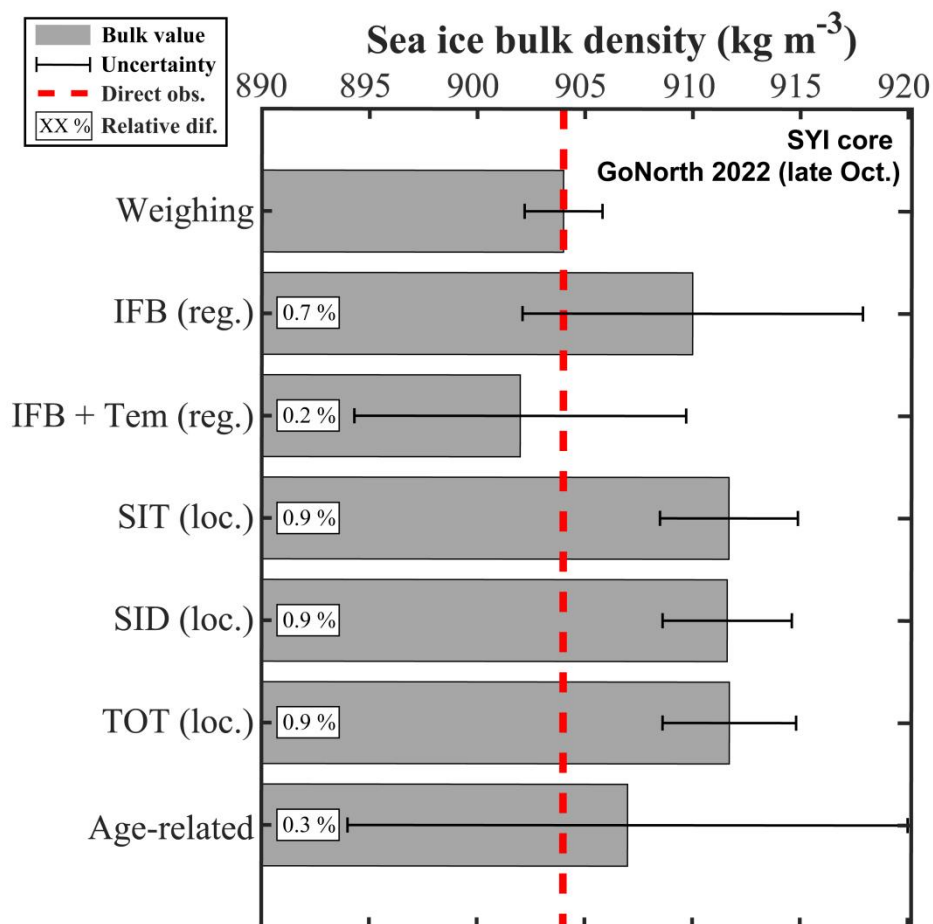


**Figure B7.** Evaluation of the regional and local IBD parameterizations during the GoNorth Expedition in late October 2022. The age-related IBD climatology and its uncertainty are also shown. **Note:** **Weighing** represents the direct measurement of IBD using the hydrostatic weighing method with an uncertainty defined as 0.2%. **Reg.** and **Loc.** are regional and local scales, respectively. **IFB**, **Tem**, **SIT**, **SID**, and **TOT** represent ice freeboard, ice bulk temperature, ice thickness, ice draft, and total thickness, respectively. The uncertainty of the IBDs derived from the parameterizations is determined by the 95 confidence intervals of their regression coefficients.



Besides, it really surprised me that in Fig. 9.a (also in 5.a) that the coring based FYI bulk density increases since October to December. Is this physical or due to sampling representations?

**GC2 Reply** We discussed in detail the possible causes of the increasing trend in IBD from late October to early December, which is mainly influenced by the air fraction (physical).

According to the theoretical relationship between the density of gas-free sea ice and its temperature and salinity (Timco and Frederking, 1996), the observed variations in bulk temperature (from about  $-4$  to  $-8$  °C) and bulk salinity (from about 6 to 5 ppt) of the FYI cores would hardly contribute to an increase in their bulk density from late October to early December (Fig. B8). Thus, the significant increase in IBD during the early stages could be closely related to the significant reduction in the air fraction (Salganik et al., 2024), as the conversion of liquid water to solid ice in closed brine pockets causes volume expansion, compressing trapped air bubbles and pushing gas into the brine solution as temperatures fall (Crabeck et al., 2016; Crabeck et al., 2019).

The rapid thickening of the sea ice may also have significantly regulated the brine volume and air fraction within the ice layer. For example, the newly formed ice layer will gradually transition from a loose granular structure to a dense columnar structure, resulting in a more compact layer (Oggier and Eicken, 2022). Indeed, the air fraction has been shown to be the most important factor influencing IBD, as it is much less dense than sea ice and brine (Timco and Frederking, 1996). Furthermore, no clear evidence of main desalination processes (Petrich and Eicken, 2017) was observed during the early phase of the study, which partly explains the relatively low IBD observed in late October. The warm air intrusion events were not shown to significantly affect sea ice bulk salinity and brine volume, although they were expected to enhance sea ice permeability, which may be related to their shorter duration (Fig. B8).

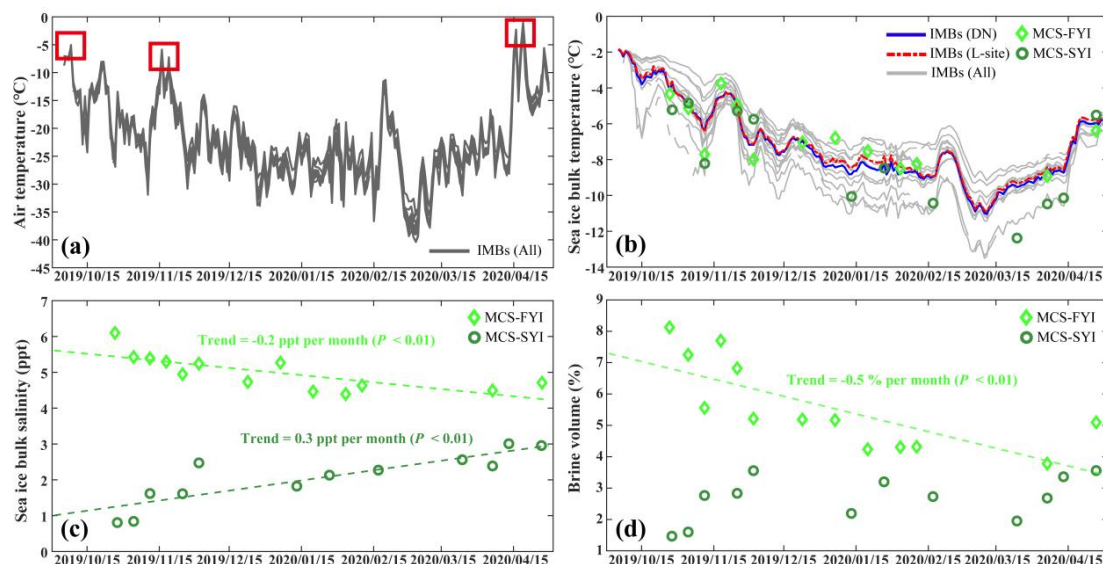


**Figure B8.** Seasonal variation of (a) buoy-derived air temperature, (b) buoy-derived and core-based sea ice bulk temperature, (c) core-based sea ice bulk salinity, and (d) core-based brine volume during the MOSAiC freezing season. The red boxes in panel (a) mark warm air intrusion events, and the dashed line in panels (c, d) indicates the seasonal linear trend ( $P < 0.01$ ).

**Our results also suggest a potential difference in ice porosity between local (MCS-SYI) and regional (SYI-dominated buoy sites) scales.** During the early period, buoy-derived mean ice thicknesses at the DN and L-site scales showed monthly growth rates of ~15 and 21 %, respectively, with the majority of buoy-monitored ice layers beginning to grow. In contrast, the MCS-SYI showed a relatively low thickness growth rate (~9 % per month) and low porosity with a brine volume of ~1 to 4 % ([Fig. B8](#)) and an air fraction of ~0.8 to 1 % (Salganik et al., 2024). In particular, Hornnes et al. (2024) found that the spatial heterogeneity of SYI porosity was greater than that of FYI during the GoNorth expedition in October 2022, and observed **similar air fractions in FYI ( $2.5 \pm 0.5$  %) and SYI cores ( $2.8 \pm 0.5$  %).**

*Second, I suggest the authors add some more discussion on the satellite altimetry. During the derivation of ice thickness with buoyancy relationship, ice bulk density is one of the model parameters. However, the IBD proposed in this work is parameterized with ice freeboard, freeboard-thickness ratio, or ice thickness. Neither of these 3 parameters are directly available for altimetry retrieval. Rather, they should be estimated with the retrieved ice thickness. Even for ice freeboard, a conversion from radar freeboard and snow data is needed, which in itself is a large unresolved issue. So I suggest that at least the detailed treatment be introduced. For example, how radar freeboard is converted into ice freeboard. The bulk density estimations (Fig. 12.c) seem to be more reasonable than AWI's default setting. But any other proof that the new IBD scheme is better than the default scheme? For example, any proof of better draft or ice thickness retrievals? Surrounding altimetry I want to mention that according to the authors the IBD scheme is developed for level ice. Although CryoSat-2 currently is not used for ice topography retrieval, ridged ice certainly plays important roles in modulating the CS2 waveform and retrieved freeboard. Is there a potential problem for applying it to the whole basin, especially given that a lot of deformed ice is present and the density estimation has potential limitations? Some discussion is suggested to be added in Sec. 4 on this issue.*

**GC3 Reply** We agree with the reviewers' suggestion and included more details on the satellite altimetry.

**1) Extended Application.** We further quantified the impact of regional IBD parameterizations (including three equations) on satellite retrievals of sea ice thickness. For this purpose, we combined satellite altimetry data, ice age field and regional IBD parameterizations (Eq. B1 and [Table B1](#)) to provide preliminary insights into the pan-Arctic SYI bulk densities and their updated thicknesses during the 2010 to 2024 freezing seasons ([Fig. B9](#)).

**2) Processing Chain.** We added details describing how to apply the regional IBD parameterizations to satellite retrievals of sea ice thickness, using the AWI CryoSat-2 sea ice thickness product (AWI CS2) as an example. Specifically, we considered the processing chain of the AWI CS2 as a benchmark, replacing its original IBD settings based on A10 climatology with the three regional IBD parameterizations (Eq. B1). **Please see details below.**

**Given the length of the main text, we provided specific details in the supplementary material**

CryoSat-2 initially provided radar backscatter data from the surface target, which can be processed to derive radar freeboard ( $h_{fr}$ ) by differentiating between ice floes and leads, as well as by retracking radar waveforms to identify the main scattering interface. Following the processing chain outlined by Hendricks and Paul (2023), the AWI CS2 algorithm includes a velocity correction term to convert radar freeboard to sea ice freeboard, taking into account the delayed radar velocity in the snow layer and assuming that the main scattering interface aligns with the snow-ice interface.

First, the CryoSat-2 sea ice freeboard can be estimated as follows:

$$h_{fi}^{cor} = h_{fr} + h_c, \quad (B3)$$

$$h_c = \left( \frac{c_v}{c_s} - 1 \right) h_s, \quad (B4)$$

where  $h_{fi}^{cor}$  is the radar velocity-corrected sea ice freeboard,  $h_{fr}$  is the radar freeboard derived using the Threshold First Maximum Retracker Algorithm (TFMRA),  $h_c$  represents the velocity correction term;  $c_v$  is the velocity of light in a vacuum ( $3 \times 10^8 \text{ m s}^{-1}$ ) and  $c_s$  is the radar propagation velocity in the snow layer. Here,  $c_s$  was obtained from a snow bulk density-dependent parameterization:  $c_s = c_v \times [1 + (5.1 \times 10^{-4})\rho_s]^{-1.5} \text{ m s}^{-1}$  (Ulaby et al., 1982);  $\rho_s$  was derived from a time-dependent equation:  $\rho_s = 6.50t + 274.51 \text{ kg m}^{-3}$  ( $t$  ranges from 0 to 6 representing October to April) (Mallett et al., 2020).

Assuming hydrostatic equilibrium, the sea ice thickness can then be determined:

$$h_i = \left( \frac{\rho_w}{\rho_w - \rho_i} \right) h_{fi}^{cor} + \left( \frac{\rho_s}{\rho_w - \rho_i} \right) h_s. \quad (B5)$$

where  $h_i$ ,  $h_{fi}^{cor}$ , and  $h_s$  represent the sea ice thickness, sea ice freeboard, and snow depth, respectively.  $\rho_w$ ,  $\rho_i$ , and  $\rho_s$  are the seawater density, sea ice bulk density, and snow bulk density, respectively. Here,  $\rho_w$  was set to  $1024 \text{ kg m}^{-3}$ ,  $\rho_s$  derived from the time-dependent equation mentioned above, and  $h_s$  was obtained from a merged snow depth product by combining W99 climatology and passive microwave measurements (MW99/AMSR2).  $\rho_i$  was configured according to the regional IBD parameterizations and the sea ice type-weighted A10 climatology (AWI original settings), respectively.

**Taking the above equations together, the unknown variables are only  $\rho_i$  and  $h_i$  when applying the regional IBD parameterizations.** For the parameterizations that depend on the sea ice freeboard or the ratio of ice freeboard to total freeboard, the IBD can be calculated directly using the individual parameters of  $h_{fi}^{cor}$  and  $h_s$  from AWI CS2. In contrast, the parameterization depending on the ratio of ice freeboard to thickness requires a combination with Eqs. (B3–5) to estimate IBD and sea ice thickness simultaneously. The final results were calculated as the mean IBD and thickness of the pan-Arctic SYI derived using all three regional IBD parameterizations (referred to as updated; [Fig. B9](#)). **Our processing details are also applicable to other CryoSat-2/ICESat-2 sea ice thickness products.**

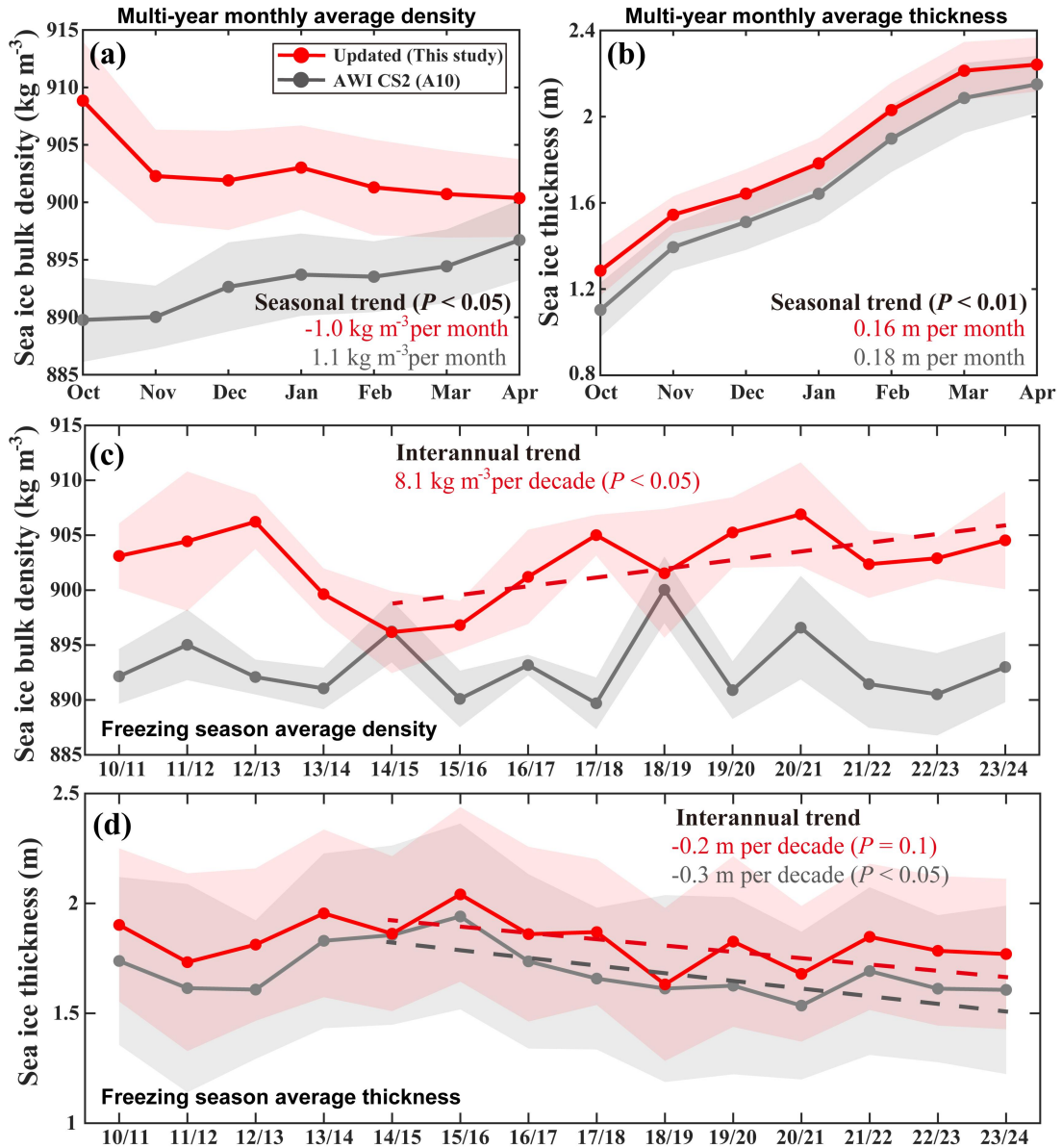


**Figure B9.** IBD and thickness variation of the pan-Arctic SYI during the 2010 to 2024 freezing seasons based on the AWI CryoSat-2 (AWI CS2) sea ice product, including results using our parameterizations (updated) and the original settings (sea ice type-weighted A10 climatology). The shaded areas denote mean  $\pm$  one standard deviation and dashed lines indicate linear trends with their statistical test  $P$ -values. **(a)** Multi-year monthly average estimates for IBD from October to April. **(b)** Multi-year monthly average estimates for ice thickness from October to April. **(c)** Freezing season average estimates for IBD from 2010/2011 (10/11) to 2023/2024 (23/24). **(d)** Freezing season average estimates for ice thickness from 2010/2011 (10/11) to 2023/2024 (23/24).

**3) Potential Improvement.** We agree with the reviewer's comment that the IBD parameterization should improve the accuracy of satellite-based sea ice thickness retrievals. However, at this stage we aim to demonstrate the validity and improvement of the regional IBD parameterization itself compared to the A10 climatology used in most sea ice thickness products, as detailed in [GCI Reply](#).

In the context of the CryoSat-2 sea ice thickness retrieval, Landy et al. (2020) demonstrated the uncertainty and contributions of various parameters in the processing chain, with IBD being only one of the key parameters. **This suggests that improvements in sea ice thickness retrieval by applying the regional IBD parameterization may be significantly influenced by other factors**, such as surface roughness, radar penetration, snow depth, and snow bulk density, leading to a bias compensation effect. In particular, both the W99-based snow depth and the assumption of full radar penetration in the snow layer used in the AWI CS2 processing chain may have contributed to an overestimation of sea ice thickness. **Therefore, we focus on reporting the impact of the regional IBD parameterization on the retrieval of sea ice thickness, highlighting the “directional changes” in its relative magnitude, seasonality and interannual variations. More importantly, the retrieved SYI bulk densities were in good agreement with the expected range and seasonal evolution.**

**In the revision, we highlight that** future incorporation of pan-Arctic SYI bulk temperatures, combined with more accurate sea ice ancillary parameters, will be more helpful in retrieving SYI bulk densities. Overall, the incorporation of regional IBD parameterizations into the current AWI CS2 product introduced more realistic variations in IBD, resulting in **systematically higher SYI thickness, lower seasonal growth rate, and reduced interannual trend.**

**4) Caveat.** We carefully discussed the impact of ice deformation on the application of our regional IBD parameterizations, which were developed solely from level ice observations.

*Added: “In terms of interpretation, the IBD at DN and L-site scales primarily reflects level ice mixed with SYI (11 buoy sites) and FYI (4 buoy sites), lacking information on other ice ages and types, particularly deformed ice, which contributes to the potential limitations and uncertainties of the parameterization scheme. Notably, deformed and unconsolidated sea ice generally exhibits a higher bulk density due to the sea water trapped within it, and applying parameterizations derived from level sea ice to satellite retrievals of sea ice thickness may consequently result in **an underestimation for deformed grid cells.**”*

**We also summarized the limitations and caveats of this study at the end of the revised manuscript:** “1) the hydrostatic equilibrium calculations of the IBD have relatively high uncertainties and sub-weekly variability compared to direct measurements; 2) the different MOSAiC observations used do not overlap spatially; 3) the regional IBD parameterizations are not strictly independent of the input parameters; 4) the IBD results represent only level sea ice and lack information on deformed ice. We can also foresee that the establishment of a regional coring network spanning different seasons and ice types will greatly advance the parameterization of IBD.”

**5) New Climatology.** Notably, both the MOSAiC and other historical records of IBD all reported higher values than the A10-MYI (up to  $\sim 30 \text{ kg m}^{-3}$ ), suggesting that the reference density used for the A10-MYI was inappropriate and may also be related to the increasing youth of Arctic sea ice. **Therefore, we proposed a new age-related IBD climatology** during the freezing season by combining the mean IBD values from the Arctic Sever expedition (Alexandrov et al., 2010; Shi et al., 2023), the IceBird campaigns (Juttila et al., 2022), and the MOSAiC expedition (this study), as shown in [Table B3](#).

**Table B3** Age-related bulk densities of level sea ice during the freezing season derived from a combination of the Arctic Sever expedition (from 1980 to 1989), the IceBird campaigns (April 2017 and 2019), and the MOSAiC expedition (from 2019 to 2020). Uncertainty is given as the maximum difference in age-related mean IBD values across observations.

Ice age	Mean ( $\text{kg m}^{-3}$ )	Standard deviation ( $\text{kg m}^{-3}$ )	Uncertainty ( $\text{kg m}^{-3}$ )
FYI (0–1 years)	916.9	7.5	20
SYI (1–2 years)	907	6.8	13
MYI (2+ years)	900	14	34

## Reference

Alexandrov, V., Sandven, S., Wahlin, J., and Johannessen, O.: The relation between sea ice thickness and freeboard in the Arctic, *The Cryosphere*, 4, 373-380, 2010.

Crabeck, O., Galley, R., Delille, B., Else, B., Geilfus, N. X., Lemes, M., Des Roches, M., Francus, P., Tison, J. L., and Rysgaard, S.: Imaging air volume fraction in sea ice using non-destructive X-ray tomography, *The Cryosphere*, 10, 1125-1145, 2016.

Crabeck, O., Galley, R. J., Mercury, L., Delille, B., Tison, J.-L., and Rysgaard, S.: Evidence of Freezing Pressure in Sea Ice Discrete Brine Inclusions and Its Impact on Aqueous-Gaseous Equilibrium, *Journal of Geophysical Research: Oceans*, 124, 1660-1678, 2019.

Hendricks, S. and Paul, S.: Product User Guide & Algorithm Specification - AWI CryoSat-2 Sea Ice Thickness (version 2.6) Issued by (v2.6), Zenodo, <https://doi.org/10.5281/zenodo.10044554>, 2023.

Hornnes, V., Salganik, E., and Høyland, K. V.: Relationship of physical and mechanical properties of sea ice during the freeze-up season in Nansen Basin, *Cold Regions Science and Technology*, 2024. 104353, 2024.

Jutila, A., Hendricks, S., Ricker, R., von Albedyll, L., Krumpfen, T., and Haas, C.: Retrieval and parameterisation of sea-ice bulk density from airborne multi-sensor measurements, *The Cryosphere*, 16, 259-275, 2022.

Landy, J. C., Petty, A. A., Tsamados, M., and Stroeve, J. C.: Sea Ice Roughness Overlooked as a Key Source of Uncertainty in CryoSat-2 Ice Freeboard Retrievals, *Journal of Geophysical Research-Oceans*, 125, 2020.

Mallett, R. D. C., Lawrence, I. R., Stroeve, J. C., Landy, J. C., and Tsamados, M.: Brief communication: Conventional assumptions involving the speed of radar waves in snow introduce systematic underestimates to sea ice thickness and seasonal growth rate estimates, *Cryosphere*, 14, 251-260, 2020.

Oggier, M. and Eicken, H.: Seasonal evolution of granular and columnar sea ice pore microstructure and pore network connectivity, *Journal of Glaciology*, 68, 833-848, 2022.

Petrich, C. and Eicken, H.: Overview of sea ice growth and properties, *Sea ice*, 2017. 1-41, 2017.

Salganik, E., Crabeck, O., Fuchs, N., Hutter, N., Anhaus, P., and Landy, J. C.: Impacts of air fraction increase on Arctic sea-ice thickness retrieval during melt season, *EGUsphere*, 2024, 1-30, 2024.

Shi, H., Lee, S.-M., Sohn, B.-J., Gasiewski, A. J., Meier, W. N., Dybkjær, G., and Kim, S.-W.: Estimation of snow depth, sea ice thickness and bulk density, and ice freeboard in the Arctic winter by combining CryoSat-2, AVHRR, and AMSR measurements, *IEEE Transactions on Geoscience and Remote Sensing*, 2023. 2023.

Timco, G. and Frederking, R.: A review of sea ice density, *Cold regions science and technology*, 24, 1-6, 1996.

Ulaby, F., Moore, R., and Fung, A.: *Microwave remote sensing: Active and passive. Volume 2-Radar remote sensing and surface scattering and emission theory*. 1982.